Marginal Fermi liquid in a lattice of three-body bound states

A. F. Ho and P. Coleman

Serin Laboratory, Rutgers University, P.O. Box 849, Piscataway, New Jersey 08855-0849

(Received 5 February 1998)

We study a lattice model for marginal Fermi-liquid behavior, involving a gas of electrons coupled to a dense lattice of three-body bound states. The presence of the bound states changes the phase space for electron-electron scattering and induces a marginal self-energy among the electron gas. When the three-body bound states are weakly coupled to the electron gas, there is a substantial window for marginal Fermi-liquid behavior and in this regime, the model displays the presence of two relaxation times, one linear, one quadratic in the temperature. At low temperatures the bound states develop coherence, leading to a crossover to conventional Fermi-liquid behavior. At strong coupling, marginal Fermi-liquid behavior is preempted by a pairing or magnetic instability, and it is not possible to produce a linear scattering rate comparable with the temperature. We discuss the low-temperature instabilities of this model and compare it to the Hubbard model at half filling. [S0163-1829(98)07232-4]

I. INTRODUCTION

The concept of a marginal Fermi-liquid (MFL) was invented as a phenomenological description of the asymptotic properties of high-temperature superconductors in their normal state.[1] These include a linear electrical resistivity $\rho \sim T$ over at least 2 decades in temperature and a quasiparticle scattering rate that may be proportional to frequency up to energies as high as 750 meV.[2,3] Even in underdoped cuprate superconductors, optical data indicate that marginal behavior develops at scales above the spin gap.[4] We shall take a marginal Fermi liquid to be a system of fermions with an inelastic scattering rate of the form

$$\Gamma \propto \max[|\omega|, T], \tag{1}$$

where there is no significant momentum dependence of Γ. In the cuprates, the constant of proportionality is of order unity. Analyticity then ensures that the appropriate self-energy takes the form

$$\Sigma(\omega) \sim \omega \ln \max[|\omega|, T]. \tag{2}$$

Many proposals have been made to explain the origin of this unusual behavior. One prevalent idea is that the marginal Fermi-liquid behavior derives from scattering off a soft bosonic mode. This idea underpins the Van Hove scenario,[5] gauge theory models,[6] and the quantum-critical scattering[7] picture of the cuprates. By contrast, Anderson[8] proposes that the cuprate metal is a fully developed Luttinger liquid, with power-law self-energies that have been misidentified as a logarithm. Since the soft-mode theories furnish an electron self-energy that is strongly momentum dependent, none of these proposals actually gives rise to a marginal Fermi-liquid as originally envisaged.

In this paper, we return to the original proposal, asking whether a marginal Fermi-liquid can form in a dense electronic system. We pursue an early speculation, due to Ruckenstein and Varma,[9] that the marginal self-energy might derive from the scattering of conduction electrons off a dispersionless localized bound state Φ at the Fermi energy, giving rise to the interaction

$$H_{\text{int}} = \lambda(c_{i\uparrow}^{\dagger} c_{i\uparrow} c_{i\downarrow}^{\dagger} \Phi + \text{H.c.}). \tag{3}$$

The presence of such states precisely at the Fermi surface would mean that the three-particle phase space grows linearly with energy. Inelastic scattering into the localized bound state then leads to a marginal self-energy in leading-order perturbation theory, as illustrated in Fig. 1. (The localized state is represented by the dashed line.) Since the hypothetical object at the Fermi surface scatters electrons in triplets, Ruckenstein and Varma identified it as a three-body bound state.

A great difficulty with this picture is that it cannot be made self-consistent. At the same level of perturbation theory that furnishes a marginal self-energy, the three-body state must scatter off the electrons to produce a self-energy term of the form shown in Fig. 2. This self-energy correction inevitably moves the resonance of the three-body bound state away from the Fermi energy, introducing an unwanted scale into the problem and causing the singular scattering to disappear.

An unexpected resolution of this problem recently appeared in the context of the single impurity two-channel Kondo model.[10] Marginal Fermi-liquid behavior does de-
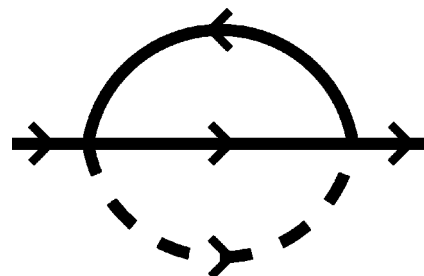

FIG. 1. Marginal self-energy diagram for the band electrons. Notation: thick lines denote band electron propagators, dashed lines denote the localized state propagator.
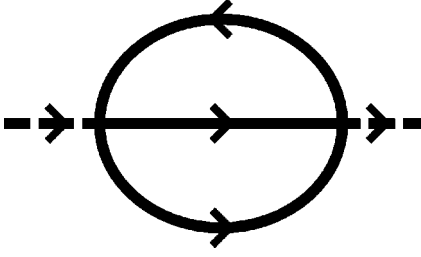

FIG. 2. Self-energy for the localized state.

velop in this model, and the mechanism by which it occurs is remarkably close to the original three-body bound state proposal, with one critical difference: in the two-channel Kondo model, the three-body bound state formed at the impurity site carries no internal quantum numbers (spin and charge). The associated bound state fermion is represented by a Hermitian operator:

$$\Phi = \Phi^{\dagger}. \qquad (4)$$

This type of fermion is known as a Majorana fermion.[11,12] The effective action for such a field must have the form

$$S = \int d\omega \Phi(-\omega)[\omega - \Sigma(\omega)]\Phi(\omega). \qquad (5)$$

Since $\Phi(-\omega)\Phi(\omega) = -\Phi(\omega)\Phi(-\omega)$ due to the Grassmanian nature of Φ, $\Sigma(\omega)$ will be an odd function of frequency, so that $\Sigma(0) = 0$. In other words, the particle-hole symmetry of the Φ field guarantees that its energy is pinned to the Fermi surface.

In the two-channel Kondo model (after dropping the charge degrees of freedom, thanks to spin-charge decoupling[13]), the total spin $\vec{S}$ of the two conduction channels at the impurity site can be written in the form $\vec{S} = -(i/2)\vec{\Psi}(0) \times \vec{\Psi}(0)$ where $\vec{\Psi} = (\Psi^{(1)}, \Psi^{(2)}, \Psi^{(3)})$ is a triplet of Majorana fermions. These three high-energy degrees of freedom bind at the impurity site to form the localized three-body bound state $\Phi(0)$, represented as the contraction of the three fermions:

$$\overline{\Psi^{(1)}(0)\Psi^{(2)}(0)\Psi^{(3)}(0)} = A\Phi(0), \qquad (6)$$

where A is the amplitude for forming this pole Φ. The residual interaction with the bulk spin degrees of freedom in the low-energy world then gives rise to a vertex of the form $\lambda \Psi^{(1)}\Psi^{(2)}\Psi^{(3)}\Phi$. The challenge here is to see if such a mechanism could be generalized to a more realistic lattice model. The work described below is an attempt to make a first step in this direction.

II. CONSTRUCTION OF MODEL

We now use these ideas to motivate a simple *lattice* model of a marginal Fermi liquid. First note that the Hubbard model at half-filling can be rewritten in a Majorana fermion representation,[14] by the following two steps. The Hubbard model is

$$H_{\text{Hubbard}} = t \sum_{i,a,\sigma} (c_{i+a,\sigma}^{\dagger} c_{i,\sigma} + \text{H.c.})$$

$$+ U \sum_{i} (c_{i\uparrow}^{\dagger} c_{i\uparrow} - 1/2)(c_{i\downarrow}^{\dagger} c_{i\downarrow} - 1/2). \qquad (7)$$

In the first step, we assume that the lattice has a bipartite structure, and do a gauge transformation on electron operators belonging to one sublattice of the bipartite lattice: $c_{i\sigma} \rightarrow -ic_{i\sigma}$. Also let the hopping term connect a sublattice A site only to a sublattice B site, and not to other sublattice A sites. Then the interaction is unchanged, but the kinetic energy becomes

$$H_{\text{KE}} = it \sum_{i,a,\sigma} (c_{i+a,\sigma}^{\dagger} c_{i,\sigma} - \text{H.c.}). \qquad (8)$$

Next, rewrite the electron operators using $c_{\uparrow} = (1/\sqrt{2})(\Psi^{(1)} - i\Psi^{(2)})$, $c_{i\downarrow} = -(1/\sqrt{2})(\Psi^{(3)} + i\Psi^{(0)})$ where the $\Psi^{(a)}$'s are Majorana fermions, and we get

$$H_{\text{Hubbard}} = it \sum_{i,c} \sum_{a=0}^{3} \Psi_{i+c}^{(a)} \Psi_{i}^{(a)}$$

$$- U \sum_{i} \Psi_{i}^{(0)} \Psi_{i}^{(1)} \Psi_{i}^{(2)} \Psi_{i}^{(3)}. \qquad (9)$$

(Note the sign change for the interaction.) In Majorana representation, we see explicitly the SO(4) symmetry[14,15] of the Hubbard model at half filling.

The crucial generalization of this paper is to break the SO(4) symmetry down to O(3), setting

$$t \rightarrow t_a = \begin{cases} t, & a = 1,2,3 \\ t_0, & a = 0. \end{cases} \qquad (10)$$

With $\Phi_i \equiv \Psi_i^{(0)}$,

$$H = it_0 \sum_{i,c} \Phi_{i+c}\Phi_i + it \sum_{i,c} \sum_{a=1}^{3} \Psi_{i+c}^{(a)} \Psi_{i}^{(a)}$$

$$- U \sum_{i} \Phi_i \Psi_{i}^{(1)} \Psi_{i}^{(2)} \Psi_{i}^{(3)}. \qquad (11)$$

When $t_0 = 0$, this Hamiltonian describes a lattice of localized three-body bound states Φ_i coupled to the continuum.

This toy model provides a simple system to study the properties of these preformed bound states at each site. A microscopic model would provide an explanation of the origin of this symmetry-breaking field, leading to the formation of these bound states. In this work, we do not address this issue, but instead ask whether the single impurity marginal Fermi-liquid mechanism survives in the lattice, in this model of reduced symmetry.

We shall show that the main physical effect of the lattice (in the absence of a broken symmetry phase) is that the previously localized mode Φ_i can now move from site to site via virtual fluctuations into the Fermi sea (see Fig. 3) thereby providing the lattice coherence energy scale $t_0 \sim U^2/t$, below which this marginal Fermi liquid reverts to a Fermi liquid. Unfortunately, this means that the marginal Fermi-liquid
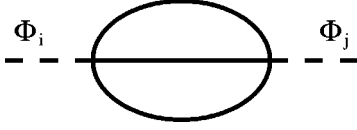
FIG. 3. Leading-order diagram that generates a dispersion for the Φ_i fermion. Note that there are no arrows on the propagator lines, as all fermions are represented by Hermitian operators.

phenomenology does not persist to large U, which makes the application of our model to the cuprates rather problematic.

To probe the marginal Fermi-liquid phenomenology, we have calculated the ''optical conductivity.'' This cannot be the ordinary electrical current, because the Hamiltonian of Eq. (15) does not conserve particle number unless $t_0 = t$ (this is most easily seen with original electron operators $c, c^\dagger$). The model does have O(3) symmetry, so there is the conserved quantity $S^a = -\frac{1}{2}\Sigma_j\Sigma^3_{\alpha,\beta=1}\Psi^{(\alpha)}_j T^a_{\alpha\beta}\Psi^{(\beta)}_j$, where T^a are the three generators of O(3). In the representation where $T^a_{\alpha\beta} = i\epsilon_{a\alpha\beta}$,

$$S^a = -\frac{i}{2}\sum_j \epsilon_{abc}\Psi^{(b)}_j\Psi^{(c)}_j. \qquad (12)$$

This leads to the conserved (Noether) current:

$$j^a_{i+\hat{x}} = it\epsilon_{abc}\Psi^{(b)}_{i+\hat{x}}\Psi^{(c)}_i. \qquad (13)$$

(See the Methods section for its derivation.) One can then define a ''conductivity'' that is the linear response of this O(3) current to an applied field. We shall show that this O(3) conductivity has the classic marginal Fermi-liquid behavior.

Within the marginal Fermi-liquid regime, the $\Psi^{(a)}$ retains its marginal self-energy. The Φ mode, while having no self-energy corrections at $T=0$ and $\omega=0$, acquires a Fermi-liquid on-site self-energy because of the virtual fluctuations into the three $\Psi^{(a)}$ (with the same diagram as Fig. 3, except that site i is the same as site j). In this regime then, our model has two distinct quasiparticle relaxation times:

$$\Gamma_\Phi = -\text{Im}\,\Sigma_\Phi(\omega) \propto \omega^2 + \pi^2 T^2, \qquad (14)$$

$$\Gamma_\Psi = -\text{Im}\,\Sigma_\Psi(\omega) \propto \max[|\omega|, T]. \qquad (15)$$

This suggests an intriguing link to the two relaxation time phenomenology observed in the electrical and Hall conductivities of the cuprates,[16] where electrical conductivity is dominated by the slower relaxation rate, while the Hall conductivity is proportional to the *product* of the two relaxation times. Unfortunately, in our model, the conserved current j^a does not include the Φ fermion, thus transport quantities constructed from this O(3) current do not reveal the slow, quadratic relaxation. We can look at another conserved quantity in our model: the total energy. Following the same strategy as for the O(3) current, it can be shown that the conserved thermal current is just a sum of currents due to each of the Φ and $\Psi^{(a)}$. Now the propagators are diagonal in the Φ or Ψ operators, thus the thermal conductivity proportional to the thermal current-current correlator will just be a sum of the relaxation times: $\kappa/T \propto 3t^2/\Gamma_\Psi + t_0^2/\Gamma_\Phi$. Also, any mixed correlators $\langle j^a Q^0 \rangle$ will be identically zero, where Q^0 is the thermal current due to Φ. In summary, it is unfortu-

nately impossible to see the two relaxation times entering *multiplicatively* in any transport quantities of our model: the various conductivities derived from the O(3) current will only depend on $\Psi^{(a)}$, whereas the thermal conductivity will be dominated by the largest relaxation time: that of the Φ fermion.

All of our previous considerations assume that the system does not develop into a broken symmetry state at low temperatures. In fact, as our Hamiltonian is a generalization of the Hubbard model at half filling, it is perhaps not surprising that it displays similar magnetic or charge ordering instabilities due to Fermi surface nesting. The main qualitative difference is the presence of a large marginal Fermi-liquid regime in the T-U phase diagram.

The plan of the paper is as follows: in Sec. III, we set out the formalism of dynamical mean field theory for solving the lattice model in the weak coupling regime. Section IV presents the results and Sec. V discusses the lattice coherence scale, and the relationship to the two-channel Kondo lattice. We also discuss the low-temperature phase of the lattice when the Fermi surface has strong nesting instability. Finally, we touch on the difficulties this model faces in modeling the cuprates.

III. METHOD

We study the Hamiltonian

$$H = i\tilde{t}_0\sum_{j,c}\Phi_{j+c}\Phi_j + i\tilde{t}\sum_{j,c}\sum^3_{a=1}\Psi^{(a)}_{j+c}\Psi^{(a)}_j$$

$$-U\sum_j \Phi_j\Psi^{(1)}_j\Psi^{(2)}_j\Psi^{(3)}_j, \qquad (16)$$

where each fermion is a canonical Majorana fermion: $\{\Psi^{(a)}_i, \Psi^{(b)}_j\} = \delta_{ab}\delta_{ij}$, $\{\Phi_i, \Phi_j\} = \delta_{ij}$, and $\{\Psi^{(a)}_i, \Phi_j\} = 0$.

To gain some insight into the properties of the model in the weak coupling limit, we use dynamical mean field theory (DMFT),[17] a method suited to systems where the dominant interaction is on-site and spatial fluctuations are unimportant, and when the on-site temporal fluctuations at all energy scales are to be taken into account. The $d\to\infty$ limit (where DMFT is exact) requires the usual scaling $\tilde{t}_a = t_a/\sqrt{d}$, with $t_a, U \sim O(d^0)$. For a lattice of localized bound states Φ_j, $\tilde{t}_0 = 0$.

The crucial simplification in DMFT is that the self-energies are k independent as any intersite diagram (such as in Fig. 3) is at most of order $1/\sqrt{d}$ relative to on-site diagrams. Now the diagram of Fig. 3 is precisely that which causes the Φ fermion to propagate: omitting it means that t_0 remains zero, and Φ_i stays localized, strictly in infinite spatial dimension. In finite d, we will need to incorporate its effect, since propagating Φ_i fields will lead to the destruction of the marginal scattering mechanism. A rigorous $1/d$ expansion appears to be formidable. Nevertheless, the essential effects of finite dimensions may be included by introducing a finite value for $\tilde{t}_0$, and treat it as a fixed parameter of the model. Defining $\tilde{t}_0 = t_0/\sqrt{d}$, we estimate t_0 by calculating the diagram (Fig. 3) in finite d at $T=0$. In Appendix A, we
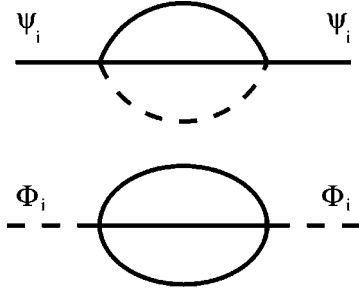
FIG. 4. On-site self-energies.

show that $t_0/t = c(U/t)^2/d$, with $t_a = t$ for $a = 1,2,3$, and c is a small constant. Finally, define a zeroth component $\Psi_j^{(0)} \equiv \Phi_j$ to get

$$H = i \sum_{j,c} \sum_{a=0}^{3} \frac{t_a}{\sqrt{d}} \Psi_{j+c}^{(a)} \Psi_j^{(a)} - U \sum_j \Psi_j^{(0)} \Psi_j^{(1)} \Psi_j^{(2)} \Psi_j^{(3)},$$

$$t_a = \begin{cases} t, & a = 1,2,3 \\ t_0, & a = 0. \end{cases} \tag{17}$$

We shall use both Φ_j and $\Psi_j^{(0)}$ interchangeably.

Following standard procedures of DMFT,[17] we map the lattice problem to an effective *single-site* problem with the effective action

$$S_{\text{eff}} = \int_0^\beta d\tau d\tau' \sum_{a=0}^{3} \Psi^{(a)}(\tau) \mathcal{G}_a^{-1}(\tau - \tau') \Psi^{(a)}(\tau')$$

$$- U \int_0^\beta d\tau (\Psi^{(0)} \Psi^{(1)} \Psi^{(2)} \Psi^{(3)})(\tau), \tag{18}$$

where $\mathcal{G}_a(\tau)$ is the dynamical mean field at the single site, which includes time-dependent influence of the rest of the lattice, and is *not* the original lattice noninteracting local Green's function. It plays the role analogous to the Weiss mean field for conventional mean field theory, and has to be determined self-consistently: see below.

The effective single-site problem dressed Green's function G is related to $\mathcal{G}$ via

$$\Sigma_a(i\omega_n) = \mathcal{G}_a^{-1}(i\omega_n) - G_a^{-1}(i\omega_n), \quad a = 0,1,2,3, \tag{19}$$

where the self-energies Σ_a are calculated from S_{eff}. To lowest order in U, they are given by the following diagrams in Fig. 4.

The effective single-site dressed Green's function must then be related back to the k average of the original lattice dressed Green's function $G_a(k, i\omega_n)$, via the mean field self-consistency equations:[17]

$$G_a(i\omega_n) = \int \frac{d^d k}{(2\pi)^d} G_a(k, i\omega_n),$$

where since in $d \to \infty$ limit, self-energies have no k dependence, $G_a(k, i\omega_n) = 1/[i\omega_n - \epsilon_a(k) - \Sigma_a(i\omega_n)]$.) Doing the integration then gives[17]

$$\mathcal{G}_a^{-1}(i\omega_n) = i\omega_n + it_a \text{sgn}(\omega_n), \quad a = 0,1,2,3 \tag{20}$$

for the Lorentzian density of state (DOS): $D_a(\epsilon) = t_a/[\pi(\epsilon^2 + t_a^2)]$ (corresponding to infinite range hopping); or alternatively

$$\mathcal{G}_a^{-1}(i\omega_n) = i\omega_n - t_a^2 G_a(i\omega_n), \quad a = 0,1,2,3 \tag{21}$$

for the semicircular DOS $D_a(\epsilon) = (1/\pi t_a)\sqrt{1 - (\epsilon/2t_a)^2}$ (corresponding to nearest-neighbor hopping on a Bethe lattice). Equations (17)–(19) and (20) or (21), and Fig. 4 together define our DMFT. The Lorentzian DOS is tractable analytically as the self-consistency equations are decoupled from G; however, this also means that the effect of the lattice enters rather trivially as just a renormalization of the bandwidth. To check these results we also use the semi-circular DOS where the self-consistency equations are solved computationally using iterated perturbation theory.[18]

One quantity of particular interest in the context of the marginal Fermi liquid is the optical conductivity. As mentioned in Sec. II, the Hamiltonian of Eq. (17) does not conserve particle number unless $t_0 = t$, thus the ordinary electrical current proportional to the particle current is not useful. We can, however, generalize the concept of the optical conductivity to this model, using the fact that the total isospin[19] $S^a = \Sigma_i(-1/2) \Psi_i^{(\alpha)} T_{\alpha\beta}^a \Psi_i^{(\beta)}$ is conserved, where $T_{\alpha\beta}^a = i\epsilon_{a\alpha\beta}$ are the O(3) generators. Combining the continuity equation: $i\partial_\tau S_i^b + \Sigma_{\hat{a}}(j_{i+\hat{a}}^b - j_i^b) = 0$ ($\hat{a}$ are the unit lattice vectors), and the equation of motion $\partial_\tau S_i^b = [H, S_i^b]$ leads to the conserved current

$$j_{i+\hat{x}}^b = it\epsilon_{b\alpha\beta} \Psi_{i+\hat{x}}^{(\alpha)} \Psi_i^{(\beta)}. \tag{22}$$

This is the Noether current associated with the O(3) symmetry of our Hamiltonian. We can then introduce a vector potential field $\vec{A}^{(a)}(\vec{x}) = (A_1^{(a)} A_2^{(a)} \cdots A_d^{(a)})$ in d-dimensional space, coupled to the electrons as follows:

$$H_A = it \sum_{i,c} \Psi_{i+c}^{(\alpha)} \exp\left\{ i \int d\vec{l} \cdot \vec{A}^{(a)} T^a \right\}_{\alpha\beta} \Psi_i^{(\beta)}, \tag{23}$$

where the line integral goes from site i to $i+c$, and a summation is implied over dummy indices. Since there is isotropy for $a = 1,2,3$, we need only study the response to the $\vec{A}^{(1)}$ component $j_x^{(1)}(\omega) = \Sigma_y \sigma_{xy}(\omega) A_y^{(1)}(\omega)$, which can be described by a Kubo formula[20]

$$\sigma_{xx}(i\omega_n) = \frac{1}{-\omega_n} \Pi(\vec{q}, i\omega_n) \bigg|_{\vec{q}=0},$$

$$\Pi(\vec{q}, i\omega_n) = -\int_0^\beta d\tau e^{i\omega_n \tau} \langle T_\tau j_x^\dagger(\vec{q}, \tau) j_x(\vec{q}, 0) \rangle.$$

In the $d \to \infty$ limit, the absence of vertex corrections to the conductivity bubble[18] permits us to write

$$\sigma(\nu_m) = \sum_{\vec{k}} T \sum_{\omega_n} (v_{k_x})^2 G_a(k, i\omega_n + i\nu_m) G_a(k, i\omega_n).$$

As usual, at temperatures much lower than the bandwidth, doing the Matsubara sum leads to a function peaking largely

near k_F, and we replace $\Sigma_{\vec{k}}(v_{k_x})^2$ by $n/m\int d\epsilon$. Doing the energy integral and analytically continuing to real frequencies:

$$\sigma(\nu+i\delta) = \frac{n}{m}\int_{-\infty}^{+\infty}d\omega\left[\frac{f(\omega_-)-f(\omega_+)}{-i\nu}\right]$$
$$\times\{\nu-[\Sigma_R(\omega_+)-\Sigma_R(\omega_-)]$$
$$+i[\Gamma(\omega_+)+\Gamma(\omega_-)]\}^{-1}, \quad (24)$$

where $\Sigma(\omega\pm i0^+)=\Sigma_R(\omega)\mp i\Gamma(\omega)$ and $\omega_{\pm}=\omega\pm\nu/2$.

IV. RESULTS

In the $d\to\infty$ limit (i.e., $t_0=0$), $\mathcal{G}_0$ is the same as the single impurity model, by Eq. (20) or (21), so the bound states described by $\Psi_i^{(0)}$ are localized, with a self-energy that has a Fermi-liquid form:

$$\Sigma_\Phi(\omega^+) = -(UN_0)^2\left\{\frac{4\omega}{\pi}+i\frac{\pi N_0}{2}[\omega^2+(\pi T)^2]\right\}, \quad (25)$$

where $\omega^+=\omega+i0^+$ and N_0 is the DOS at the Fermi surface. We give a brief derivation of this result in Appendix B. For $\Psi_i^{(a)}$, $a=1,2,3$, the mean field $\mathcal{G}_a$ of the effective single site problem is of the same form as the single impurity model bare Green's function, using the Lorentzian DOS for the $d\to\infty$ lattice. This is due to the DOS in the effective problem being smooth at Fermi energy, and for $T\ll t$, equaling a constant N_0, just as in the single-impurity model.[10] We then obtain the marginal self-energy:

$$\Sigma_\Psi(\omega^+) = -(UN_0)^2\omega\left[\ln\frac{\Lambda}{T}-\Psi\left(1-\frac{i\omega}{2\pi T}\right)+\frac{\pi T}{i\omega}\right], \quad (26)$$

where Λ is a cutoff proportional to t, Ψ is the digamma function, $\gamma\sim0.6$ is the Euler constant (Appendix B). This has the following limiting behavior

$$\Sigma_\Psi(\omega^+) = (UN_0)^2$$
$$\times\begin{cases}(-\omega\ln2\pi\Lambda/|\omega|-i(\pi/2)|\omega|) & (\omega\gg T)\\(-\omega\ln\Lambda e^\gamma/T-i\pi T) & (\omega\ll T).\end{cases} \quad (27)$$

At finite d, the lattice coherence energy scale t_0 generated from the diagram of Fig. 3 becomes finite, with $t_0\sim U^2/t$. Marginal Fermi-liquid behavior will now persist so long as $t_0<T\ll t$. At lower temperatures $T\ll t_0<t$ the three-body bound states begin to propagate coherently, causing a crossover to Fermi-liquid behavior. This is borne out by analytical calculations; here we illustrate with computational results (using the semicircular DOS) in Fig. 5 showing the effective quasiparticle scattering rate $\Gamma(\omega)=\omega$ Re $\sigma(\omega)/\text{Im }\sigma(\omega)\sim -\text{Im }\Sigma_\Psi(\omega^+)$, where $\sigma(\omega)$ is the optical conductivity defined in the Methods section. In Fig. 6 we plot the resistivity $\rho(T)$ showing the large linear T regime at weak coupling, and the inset shows the crossover to the T^2 Fermi-liquid regime.
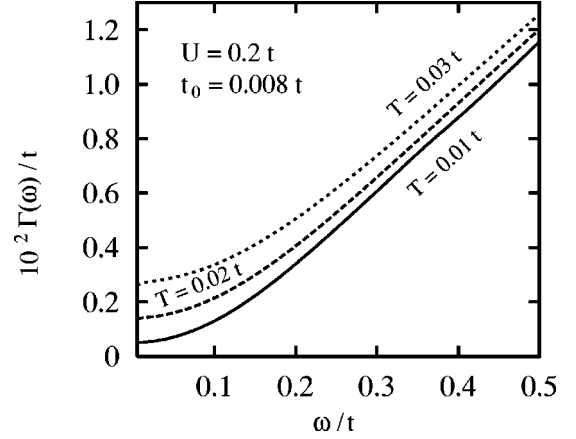

FIG. 5. Plot of quasiparticle scattering rate $\Gamma(\omega)$ $=\omega$ Re $\sigma/\text{Im }\sigma$.

V. DISCUSSION AND CONCLUSION

In this paper we have shown how a lattice of three-body bound states induces marginal Fermi-liquid behavior above a lattice coherence temperature t_0 where a Fermi liquid forms. Since $t_0\sim U^2/t$, a substantial window in temperature for marginal Fermi-liquid behavior exists only for small U. The emergence of this lattice coherence energy is expected to be quite general: whenever a localized mode is allowed to interact with conduction electrons, it will be difficult to prevent hybridizations between fields at different sites. These effects, however, are missed in a strict $d\to\infty$ calculation.[21]

This brings us to the question of the relationship between our lattice model and the two-channel Kondo lattice model. The single-impurity version of the Hamiltonian of Eq. (11) (with $U<0$) was originally derived[10] in the context of the single-impurity two-channel Kondo model.[22] That derivation took advantage of spin-charge separation[13] to throw away uncoupled (charge) degrees of freedom, and it has been shown via bosonization to be exactly equivalent to the original model.[23] Unfortunately there is no such relation between
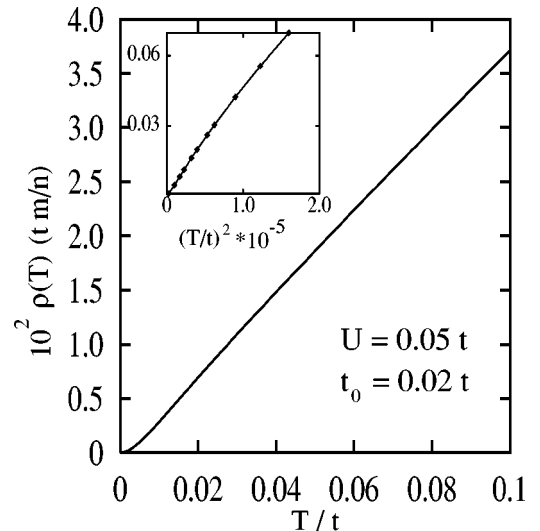

FIG. 6. Plot of resistivity vs T. Inset shows the very low-temperature crossover to T^2 behavior: the y axis is in the same units as the big plot.

the two-channel Kondo lattice[24] and the Majorana lattice considered here.

Also, we should point out that in the single-impurity two-channel Kondo model, while the self-energy for the band Majorana fermions has the marginal Fermi-liquid form and dominates the thermodynamics, the physical band electrons actually have a leading frequency dependence $\sim \omega^{1/2}$, and this shows up in the electrical resistivity having a $T^{1/2}$ leading temperature dependence.[25] This comes about due to the highly nonlinear transformations of the original physical electrons to get to the Majorana fermions (bosonization and refermionization). Our O(3) lattice model, while motivated by the single-impurity two-channel Kondo model, is *not* derived from the lattice two-channel Kondo model. Here we consider our model as a low-energy effective theory of as yet unknown microscopic origin, and as such we cannot address the issue of how the Majorana fermions are related to the microscopic degrees of freedom.

In the above calculations, we have assumed that the marginal Fermi-liquid state is unstable only to the Fermi-liquid state at low T. In fact, just as in the Hubbard model, a mean-field calculation indicates that for a Fermi surface with a strong nesting instability (for example, nearest-neighbor hopping in a hypercubic lattice), there is a phase transition to antiferromagnetic order (for $U>0$). The order parameter is a vector that reflects the O(3) symmetry of the model:

$$V^a(\vec{x}_j) = e^{iQ\cdot x_j}\langle c_\alpha^\dagger \sigma_{\alpha\beta}^a c_\beta\rangle$$

$$= ie^{iQ\cdot x_j}\langle \Psi^{(0)}\Psi^{(a)} - \tfrac{1}{2}(\vec{\Psi}\times\vec{\Psi})^a\rangle, \qquad (28)$$

where $Q=(\pi,\ldots,\pi)$ is the nesting vector. From the divergence in the susceptibility, we find that at weak coupling, $T_c < t_0$, except when $t_0 = 0$:

$$\frac{T_c}{\Lambda} = \exp\left[\frac{\ln t_0/t}{4} - \sqrt{\frac{(\ln t_0/t)^2}{4} + \frac{1+t_0/t}{2(UN_0)^2}}\right], \quad (29)$$

where Λ is a cutoff ($\Lambda < t$). (Note that this reduces to the Hubbard model value when $t_0 = t$.) At $t_0 = 0$, T_c is identical to the Hubbard case. For $0 < t_0 < t$, T_c is enhanced relative to the Hubbard case. Hence a region of Fermi-liquid phase separates the low-temperature antiferromagnetic phase from the marginal Fermi-liquid regime: see Fig. 7.

There are further similarities to the Hubbard model at half filling. Both the SO(4) and O(3) models are invariant under $U\to -U$ and $\Psi^{(0)}\to -\Psi^{(0)}$. The latter map corresponds to a particle-hole transformation for the down spin only: $c_\downarrow \leftrightarrow c_\downarrow^+$. This implies that in going from the positive U model to the negative U model, magnetic ordering turns into charge ordering.[26] It can also be shown that neither model mixes charge and magnetic ordering. Further, both models reduce to the Heisenberg antiferromagnet as $U\to\infty$. Thus our model has very similar properties to the half-filled Hubbard model, except for the marginal Fermi-liquid phase at weak coupling.

What insight does our model bring towards the understanding of the marginal Fermi-liquid behavior in the cuprates? While our model does provide a simple lattice realization of a marginal Fermi liquid, it unfortunately suffers from a number of defects, listed as follows.
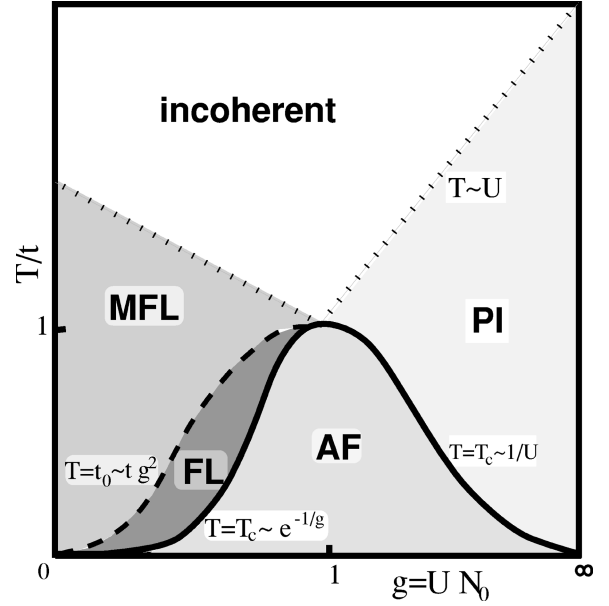

FIG. 7. Schematic phase diagram of the Majorana lattice model. The dimensionless coupling is $g\equiv UN_0$ where $N_0\propto 1/t$ is the density of states at the Fermi surface. $t_0 = ctg^2/d$. MFL is the marginal Fermi-liquid phase, FL is the Fermi-liquid phase. AF is the antiferromagnetic phase, PI is the paramagnetic insulating phase. At weak coupling, T_c goes as $\exp(-1/g)$, while at strong coupling, it goes as t^2/U. We have no computation for strong coupling for $T>T_c$, thus we do not know the continuation of the $T=t_0$ line. However, we might expect that when U is of order t, T_c and t_0 will also be of order t. One scenario is then the $T=t_0$ line meets and ends at the $T=T_c$ line around t_0. Also, at strong coupling, the paramagnetic insulator crosses over to a metal at $T\sim U$ (in analogy to the Hubbard model), and in the weak coupling regime, there will be a similar high-temperature crossover from marginal Fermi liquid to an incoherent metallic phase: these crossovers are indicated with a dotted line.

(i)   It has a wide window of marginal Fermi-liquid behavior only for small coupling. The cuprates are believed to be in the strong coupling regime,[27] but at strong coupling, our system has charge or magnetic instabilities. Related to this is the fact that in the cuprates, the inelastic scattering rate $\Gamma = \Gamma_0 \max[\omega, T]$ has Γ_0/t a constant of order one, whereas our model has Γ_0/t proportional to the coupling squared.

(ii)   The model needs to be at half filling: upon doping, a chemical potential term $\mu(\Psi^{(0)}\Psi^{(3)} + \Psi^{(1)}\Psi^{(2)})$ leads to a width $\Delta\propto\mu^2$ for Φ, with Fermi-liquid properties when $T<\Delta$. This seems to require fine tuning, contradicting the rather robust linear-T resistivity observed even in underdoped systems (above the ''spin gap'' scale).

(iii) Despite the presence of two relaxation rates in the system, transport quantities will not involve a multiplicative combination of the Φ and Ψ relaxation rates, as is postulated in the two-relaxation-times phenomenology for the cuprates. (See Sec. II.)

In conclusion we have demonstrated the persistence of marginal Fermi-liquid behavior at weak coupling in a toy

model of a marginal Fermi-liquid in an infinite-dimensional lattice. For finite d, the lattice coherence energy cuts off marginal Fermi-liquid behavior and the system reverts to a Fermi liquid at low temperatures. Since this cut-off grows with the coupling, there will be no marginal Fermi-liquid regime at strong coupling. It remains to be seen if a strong coupling marginal Fermi liquid exists in any finite dimensions.

ACKNOWLEDGMENTS

APPENDIX A: CALCULATION OF THE EFFECTIVE BANDWIDTH t_0

We want to estimate in finite dimensions the effective kinetic energy $i\tilde{t}_0 \Sigma_{i,c} \Psi_{i+c}^{(0)} \Psi_i^{(0)}$ from the zero-frequency part of the $\Psi^{(0)}$ self-energy, as depicted in Fig. 3, to lowest order in the coupling:

$$i\tilde{t}_0 = U^2 \int_0^\beta d\tau [G_{\hat{x}}(\tau)]^3, \quad (A1)$$

where $G_{\hat{x}}(\tau)$ is the bare propagator of $\Psi^{(a)}(a=1,2,3)$, for nearest-neighbor sites, taken here to be in the $\hat{x}$ direction. In k,ω space, $G(\vec{k},i\omega_n)=[i\omega_n-\epsilon_{\vec{k}}]^{-1}$. For simplicity, take $\epsilon_{\vec{k}}=-2\tilde{t}\Sigma_{i=1}^d \sin(k_i)$, appropriate for the hypercubic nearest-neighbor dispersion. (We expect that as $T\to 0$, the exact shape for the band does not matter.) Let $\tilde{t}=t/\sqrt{d}$ and $\tilde{t}_0 = t_0/\sqrt{d}$, as required for a proper scaling of the kinetic energy term in large d limit. Then $G_{\hat{x}}(\tau)$ will be of order $1/\sqrt{d}$, and as mentioned in the Methods section, $\tilde{t}_0 \sim O(d^{-3/2})$, i.e., $1/d$ down on the dispersion for the $a=1,2,3$ components. Doing the standard Matsubara sum leads to

$$G_{\hat{x}}(\tau) = \int \frac{d^d k}{(2\pi)^d} f(-\epsilon_{\vec{k}})\exp(i\vec{k}\cdot\hat{x}-\epsilon_{\vec{k}}\tau). \quad (A2)$$

In the zero-temperature limit, the Fermi function become $f(-\epsilon_{\vec{k}})\to\theta(\epsilon_{k_x}+\epsilon_{\vec{k}}')$, where we have split up the dispersion into the k_x part and the other $d-1$ part. Turning the $(d-1)$-dimensional k integral into an energy integral gives

$$G_{\hat{x}}(\tau) = \int \frac{dk_x}{(2\pi)} e^{ik_x-\epsilon_{k_x}\tau} \int_{-\epsilon_{k_x}}^\infty d\epsilon\, N(\epsilon)e^{-\epsilon\tau}, \quad (A3)$$

where $N(\epsilon)$ is the density of states in $d-1$ dimensions.

To make further progress, a flat density of states is used: $N(\epsilon)=1/(4t)$ for $|\epsilon|<2t$ and zero otherwise. Thus, defining the dimensionless time variable $s=2\tau t$,

$$G_{\hat{x}}(s) = -\frac{e^{-s}}{2s} J_1\left(i\frac{s}{\sqrt{d}}\right), \quad (A4)$$

where $J_1(z)=\int_{-\pi}^\pi (dx/2\pi) e^{-iz\sin(x)+ix}$ is the Bessel function of the first kind of the first order. Thanks to the factor of $1/\sqrt{d}$ inside its argument, the Bessel function asymptotically always grows more slowly than the decay due to the e^{-s} factor. [For $|\arg(z)|<\pi$ and $|z|\to\infty$, $J_1(z)\to(2/\pi z)^{1/2}\cos(z-3\pi/4)$.] Thus, contributions to the integral in Eq. (A1) are dominated by the regime when the Bessel function is at most of order one, allowing us to approximate $iJ_1(ix)=-x/2+O(x^3)$ in Eq. (A4), leading finally to

$$\tilde{t}_0 \simeq \frac{U^2}{2t}\int_0^\infty ds\left[\frac{e^{-s}}{2s}\frac{s}{2\sqrt{d}}\right]^3 = \frac{U^2}{2^7\times 3td^{3/2}}, \quad (A5)$$

with $\tilde{t}_0$ of order $d^{-3/2}$ as claimed.

APPENDIX B: CALCULATION OF THE MARGINAL SELF-ENERGY

To order U^2, the on-site self-energy for $\Psi_i^{(a)}$, $a=1,2,3$ is

$$\Sigma_\Psi(\tau) = U^2 \mathcal{G}_0(\tau)\mathcal{G}_a(\tau)\mathcal{G}_a(\tau). \quad (B1)$$

$\mathcal{G}_0(\tau)=\text{sgn}(\tau)/2$ is identical to the single impurity $\Psi^{(0)}$ propagator,[10] since in the strict $d\to\infty$ limit, $t_0=0$. For $\Psi_i^{(a)}$,

$$\mathcal{G}_a(\tau) = T\sum_{\omega_n} \frac{e^{-i\omega_n\tau}}{i\omega_n+it_a\text{sgn}(\omega_n)} \quad (B2)$$

where we have used Eq. (20) for $\mathcal{G}_a(i\omega_n)$ for the Lorentzian DOS. As usual, turn the Matsubara sum into a contour integral and deform the contour onto the branch cut at the real axis to get

$$\mathcal{G}_a(\tau) = -\text{Im}\int_{-\infty}^\infty \frac{d\omega}{\pi}[1-f(\omega)]\frac{e^{-\omega\tau}}{\omega+it_a}. \quad (B3)$$

[$f(\omega)$ is the Fermi function.] As we are interested in $T\ll t_a$, the integrand is dominated by small ω, and we approximate the denominator $\omega+it_a\approx it_a$. Now the d-dimensional Lorentzian DOS at the Fermi surface is $N_0=1/(\pi t_a)$, and thus $\mathcal{G}_a(\tau)$ is identical to that for the single-impurity calculation:[10]

$$\mathcal{G}_a(\tau) = \frac{N_0\pi T}{\sin(\tau\pi T)}. \quad (B4)$$

Note that this expression is accurate for $0\ll\tau\ll\beta$. Going to Matsubara frequencies $\omega_n=(2n+1)\pi T$:

$$\Sigma_\Psi(i\omega_n) = U^2\int_0^\beta d\tau \frac{\text{sgn}(\tau)}{2}\left(\frac{N_0\pi T}{\sin(\tau\pi T)}\right)^2 e^{-i\omega_n\tau}$$

$$= -i\frac{\pi T}{2}(UN_0)^2 I_n(\epsilon) \quad (B5)$$

where

$$I_n(\epsilon) = \int_\epsilon^{\pi-\epsilon} dx \frac{\sin(2n+1)x}{[\sin(x)]^2}. \quad (B6)$$

We have put in a cutoff $\epsilon = \pi T/(2t_a) \ll 1$. Integrating by parts twice, and using the tabulated integral:[28] $\int_0^\pi dx \ln \sin(x)\sin(2n+1)x = -[2/(2n+1)][1/(2n+1)+\ln 2 + \gamma + \Psi(n+1/2)]$, we get

$$I_n(\epsilon) = \frac{2\omega_n}{\pi T}\left[\ln\left(\frac{\Lambda}{T}\right) - \Psi\left(\frac{\omega_n}{2\pi T}\right)\right] - 2. \quad (B7)$$

$\Psi(x)$ is the digamma function, $\Lambda = t_a e^{1-\gamma}/(\pi T)$ and $\gamma \sim 0.6$ is the Euler constant. (We have expanded in ϵ and kept only the terms up to ϵ^0.) Putting this all together and performing the analytic continuation $i\omega_n \to \omega + i0^+$ gives Eq. (26).

The on-site self-energy for Φ is

$$\Sigma_\Phi(\tau) = U^2 \mathcal{G}_a(\tau)\mathcal{G}_a(\tau)\mathcal{G}_a(\tau). \quad (B8)$$

Fourier transforming,

$$\Sigma_\Phi(i\omega_n) = iN_0(N_0 U\pi T)^2 K_n, \quad (B9)$$

$$K_n = \int_\epsilon^{\pi-\epsilon} dx \frac{\sin(2n+1)x}{[\sin(x)]^3}.$$

Again, we have a cutoff $\epsilon = \pi T/(2t_a) \ll 1$. Integrating by parts and expanding in ϵ, $K_n = 2(2n+1)/\epsilon - 2n(n+1)\pi$. This then leads to Eq. (25) after analytic continuation.

[1] C. M. Varma, P. B. Littlewood, S. Schmitt-Rink, E. Abrahams, and A. E. Ruckenstein, Phys. Rev. Lett. **63**, 1996 (1989).

[2] Z. Schlesinger *et al.*, Phys. Rev. Lett. **65**, 801 (1990).

[3] A. El Azruak, R. Nahoum, N. Bontemps, M. Guilloux-Viry, C. Thivet, A. Perrin, S. Labdi, Z. Z. Li, and H. Raffy, Phys. Rev. B **49**, 9846 (1994).

[4] A. V. Puchkov, D. N. Basov, and T. Timusk, J. Phys.: Condens. Matter **48**, 10 049 (1996).

[5] J. E. Hirsch and D. J. Scalapino, Phys. Rev. Lett. **56**, 2732 (1986); D. M. Newns, *et al.*, *ibid.* **73**, 1695 (1994). For further references, see the review R. S. Markiewicz, cond-mat/9611238 (unpublished).

[6] L. B. Ioffe and A. I. Larkin, Phys. Rev. B **39**, 8988 (1989); G. Kotliar, *ibid.* **37**, 3664 (1989); P. A. Lee and N. Nagaosa, *ibid.* **46**, 5621 (1992).

[7] A. Sokol and D. Pines, Phys. Rev. Lett. **71**, 2813 (1993).

[8] For the most recent and comprehensive review of Anderson's thinking, see P. W. Anderson, *The Theory of Superconductivity in the High T_c Cuprates* (Princeton University Press, Princeton, NJ, 1997).

[9] A. E. Ruckenstein and C. M. Varma, Physica C **185–189**, 134 (1991).

[10] P. Coleman, L. Ioffe, and A. M. Tsvelik, Phys. Rev. B **52**, 6611 (1995).

[11] E. Majorana, Nuovo Cimento **14**, 171 (1937). Such an object can always be constructed as a linear combination of two charged fermions $\Phi = (1/\sqrt{2})(a+a^\dagger)$.

[12] P. Coleman, E. Miranda, and A. M. Tsvelik, Phys. Rev. Lett. **74**, 1653 (1995).

[13] V. J. Emery and S. Kivelson, Phys. Rev. B **46**, 10 812 (1992).

[14] I. Affleck, in *Physics, Geometry, and Topology*, Vol. 238 of NATO Advanced Study Institute, Series B: Physics, edited by H. C. Lee (Plenum, New York, 1990).

[15] C. N. Yang and S. C. Zhang, Mod. Phys. Lett. B **4**, 759 (1990).

[16] P. W. Anderson, Phys. Rev. Lett. **67**, 2092 (1991); P. Coleman, A. J. Schofield, and A. M. Tsvelik, J. Phys.: Condens. Matter **8**, 9985 (1996).

[17] See the review of A. Georges, G. Kotliar, W. Krauth, and M. J. Rozenberg, Rev. Mod. Phys. **68**, 13 (1996). All other technical points about MFT mentioned in our paper is explained in detail here.

[18] A. Georges and G. Kotliar, Phys. Rev. B **45**, 6479 (1992). We modify their algorithm slightly by doing the self-consistency loop with the spectral weights $\rho_a(\omega) = -(1/\pi)\text{Im } G_a(i\omega_n \to \omega + i0^+)$ rather than $G(i\omega_n)$, and the self-consistency equations become $\rho_a(\omega) = (1/\pi t_a)\{\text{Im }\Sigma(\omega+i0^+)/t + \text{Im}\sqrt{\{[\omega-\Sigma(\omega+i0^+)]/t_a\}^2 - 2}\}$.

[19] This is the Majorana [O(3)] representation of a spin-1/2 operator, see, e.g., D. C. Mattis, *The Theory of Magnetism I* (Springer-Verlag, Berlin, 1988); and A. M. Tsevlik, *Quantum Field Theory in Condensed Matter Physics* (Cambridge University Press, Cambridge, 1995).

[20] See, e.g., G. D. Mahan, *Many Particle Physics* (Plenum, New York, 1991).

[21] We have done a $d=2$, order U^2 calculation of the imaginary part of the self-energy Σ_Ψ to check explicitly our large d results. To avoid complications from nesting or Van Hove singularities, we used a circular Fermi surface. We find to leading order in ω and in $t/t_0 \gg 1$ that at $T=0$, $\text{Im}\Sigma_\Psi \sim (U^2/t)(t/t_0)\omega^2 \ln[(t/t_0)\omega]$, which is indeed the $d=2$ Fermi-liquid result. The calculation proceeds in the same way as in the weak-coupling Hubbard model, see, e.g., C. Hodges, H. Smith, and J. W. Wilkins, Phys. Rev. B **4**, 302 (1971).

[22] P. Nozières and A. Blandin, J. Phys. (Paris) **41**, 193 (1980).

[23] A. J. Schofield, Phys. Rev. B **55**, 5627 (1997); G.-M. Zhang, A. C. Hewson, and R. Bulla, cond-mat/9705199, 1997 (unpublished).

[24] For a large-d treatment of the two-channel Kondo lattice, see M. Jarell, H. Pang, D. L. Cox, F. Anders, and A. Chattopadhyay, cond-mat/9609146, 1996 (unpublished); D. L. Cox and M. Jarell, J. Phys.: Condens. Matter **8**, 9825 (1996). It should be noted that our model here, although inspired by the compactified version of the single impurity two-channel Kondo model, bears *no* simple relation to the two-channel Kondo lattice.

[25] I. Affleck and A. W. W. Ludwig, Phys. Rev. B **48**, 727 (1993), see also a detailed discussion of this point in the review D. L. Cox and A. Zawadowski, cond-mat/9704103, 1997 (unpublished).

[26] This is well known for the Hubbard model, see, e.g., E. Fradkin, *Field Theories in Condensed Matter Systems* (Addison-Wesley, New York, 1991).

[27] See, e.g., M. S. Hybertsen, M. Schlüter, and N. E. Christensen, Phys. Rev. B **39**, 9028 (1989). They estimated U on copper sites to be around 10.5 eV, versus oxygen-copper hopping $\sim$1.3 eV.

[28] I. S. Gradshteyn and I. M. Ryzhik, *Table of Integrals, Series, and Products*, 5th ed. (Academic Press, London, 1994), No. 4.384.2.